AD-A160 622 MECHANICAL PROPERTIES OF SIC FIBER-REINFORCED REACTION-BONDED SI3N4 COMPOSITES(U) NATIONAL AERONAUTICS AND SPACE ADMINISTRATION CLEVELAND OH LE.. 1/1

UNCLASSIFIED R T BHATT 1985 NASA-E-2671 NASA-TM-87085 F/G 11/4 NL

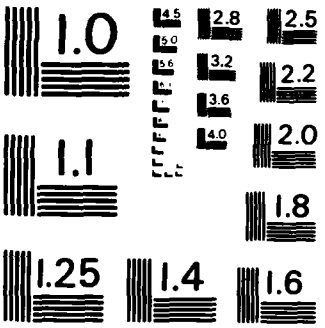

MICROCOPY RESOLUTION TEST CHART
NATIONAL BUREAU OF STANDARDS - 1963 - A

NASA
Technical Memorandum 87085

USAAVSCOM
Technical Report 85-C-14

Mechanical Properties of SiC Fiber-Reinforced Reaction-Bonded Si_3N_4 Composites

Ramakrishna T. Bhatt
Propulsion Directorate
U.S. Army Aviation Research and Technology Activity (AVSCOM)
Lewis Research Center
Cleveland, Ohio

Prepared for the
21st University Conference on Ceramic Science
sponsored by The University of Pennsylvania
University Park, Pennsylvania, July 17-19, 1985

NASA

MECHANICAL PROPERTIES OF SiC FIBER-REINFORCED REACTION-BONDED Si_3N_4 COMPOSITES

Ramakrishna T. Bhatt
Propulsion Directorate
U.S. Army Aviation Research and Technology Activity (AVSCOM)
NASA Lewis Research Center
Cleveland, Ohio 44135

SUMMARY

The room temperature mechanical and physical properties of silicon carbide fiber-reinforced reaction-bonded silicon nitride composites (SiC/RBSN) have been evaluated. The composites contained ~23 and ~40 volume fraction of aligned 140 μm diameter chemically vapor deposited SiC fibers. Preliminary results for composite tensile and bend strengths and fracture strain indicate that the composites displayed excellent properties when compared with unreinforced RBSN of comparable porosity. Fiber volume fraction showed little influence on matrix first cracking strain but did influence the stresses required for matrix first cracking and for ultimate composite fracture strength. It is suggested that by reducing matrix porosity and by increasing the volume fraction of the large diameter SiC fiber, it should be possible to further improve the composite stress at which the matrix first cracks.

INTRODUCTION

Because of their lightweight, excellent oxidation resistance, high temperature strength, environmental stability, and nonstrategic nature, silicon-based ceramics are candidate materials for high performance advanced gas turbine and diesel engines. However, the use of these materials is severely limited because of their inherent flaw sensitivity and brittle behavior. Past studies (refs. 1 and 2) have shown that reinforcement of ceramics by high strength, high modulus, continuous length ceramic fibers should yield stronger and tougher materials. Glass matrix composites reinforced by polymer derived silicon carbide fibers (Nicalon) (ref. 3) have clearly demonstrated the feasibility of obtaining strong and tough materials. These newly developed composites, however, are presently limited in temperature capability by matrix properties, interfacial reactions, and by thermal instability of the fibers above about 1000 °C.

In contrast, the present study reports the development of a strong and tough ceramic matrix composite which should have potential for use in advanced engines operating at temperatures above 1200 °C. In this study, silicon carbide fiber-reinforced reaction-bonded Si_3N_4 (SiC/RBSN) composites were fabricated and their physical and mechanical properties determined. The study was performed to obtain basic understanding about the reinforcing effects of fibers, fiber interaction with the matrix, and fiber strength stability under processing conditions. Wherever possible, metallographic and fractographic analyses were also performed to study microstructure and failure mechanisms.

EXPERIMENTAL

Fiber

The SiC fibers used in this study were obtained from AVCO Specialty Materials Division. These fibers were produced by chemical vapor deposition (CVD) from methyl trichlorosilane onto a heated carbon monofilament which was pulled continuously through the deposition reactor (ref. 4). Different surface coatings were deposited onto the SiC fibers by introducing hydrocarbon gas or a mixture of hydrocarbon gas and silane vapor near the exit port of the reactor. A schematic diagram of the fiber cross section is shown in figure 1(a). The fiber consists of a SiC sheath with an outer diameter of 142 μm surrounding a pyrolytic graphite coated carbon core with diameter of 37 μm (1.3 mil). The SiC sheath is entirely comprised of columnar β-SiC grains growing in a radial direction with {111} preferred direction (ref. 4). The fiber used for composite fabrication contained a surface coating consisting of an overlayer with high silicon/carbon ratio on top of an amorphous carbon layer (cf. fig. 1(b)). The total thickness of the coating is ~2 μm. This type of fiber, labeled SCS-6 by the manufacturer, was originally developed for metal matrix composites. The average room temperature tensile strength of the as-received SCS-6 fibers was 3.8 GPa (gauge length = 50 mm).

Ceramic Powder

High purity silicon powder was used for preparation of the reaction-bonded Si_3N_4 matrix. The impurity content of the as-received powder is shown in table I. This powder contained a high volume fraction of large particles (>20 μm) which are even larger than the interfiber distance of the desired composites. To reduce particle size and to promote reactivity during nitridation, the silicon powder was attrition milled for several hours in a Si_3N_4 container using Si_3N_4 balls and heptane solvent. After milling, the excess solvent was evaporated from the powder. The powder was then dried and stored for use in composite fabrication. The chemical analysis, average surface area, and particle size of the powder before and after attrition milling are shown in table II. It is obvious from the table that after attrition milling there was a significant increase in the oxygen and carbon contents and essentially no increase in iron content. The surface area of the powder increased from 1 m^2/g to 10 m^2/g while the average particle size decreased from 6 μm to 0.4 μm.

Composite Fabrication

The SiC/Si_3N_4 matrix composite material was consolidated by a method similar to that employed for fiber-reinforced metal matrix composites (ref. 5). The details of the fabrication process will be reported elsewhere (ref. 6).

To describe the fabrication method briefly, the SiC fiber was wound with desired spacing on a circular drum and coated with a slurry consisting of attrition milled silicon powder, an additive (for enhancing nitridation), a fugitive polymer binder, and a solvent. After carefully drying the fiber mat, it was cut into strips of required dimensions. These strips were stacked up in a graphite die and hot pressed in vacuum or in a nitrogen environment at a suitable combination of temperature and pressure to produce handleable green

compacts. Using this method, two types of composite green compacts were produced. One contained ~23 volume fraction and the other ~40 volume fraction of SiC fibers. The volume fraction of fibers in the green compact was varied by controlling fiber spacing or by adjusting the thickness of the silicon slurry. Before further processing, the green compacts were weighed and their densities and porosity measured by a mercury porosimeter.

The green compacts were then transferred to a horizontal nitridation furnace consisting of a recrystallized Al_2O_3 reaction tube with stainless steel end caps. The compact loading and furnace description were the same as reported in reference 7. The nitriding gas (N_2 or N_2 + 4 percent H_2) of commercial purity was purified according to the procedure followed in reference 7 and then flowed through the furnace before, during, and after nitridation. The nitriding temperature and nitriding schedule for the composite were similar to that employed for monolithic reaction-bonded silicon nitride (ref. 8). Upon completion of nitridation, the composite plates were reweighed and their densities measured. The nitrided composite materials were examined by x-ray diffraction using the technique developed by Gazzara and Messier (ref. 9) to determine the amount of αSi_3N_4, βSi_3N_4, and residual silicon.

Specimen Preparation

The as-fabricated nitrided composite plates contained excess matrix layer on their top and bottom surfaces. This matrix layer was removed by grinding the composite plate on SiC papers. Specimens for mechanical testing were prepared from the composite plates by cutting and grinding with a diamond impregnated abrasive wheel. For three-point bend tests, typical specimen dimensions were 50 by 6.4 by 1.2 mm, and the span to height ratio (L/h) was 35. For four-point bend tests, typical specimen dimensions were 63.5 by 6.4 by 1.2 mm for (L/h) = 45 and 31.8 by 6.4 by 1.2 mm for (L/h) = 15. Maximum bend stresses were calculated assuming a homogeneous microstructure for the composites. For tensile tests, specimens of dimensions 127 by 12.7 by 1.2 mm were adhesively bonded with glass fiber-reinforced epoxy tabs at the specimen ends, leaving 50 mm as the test gauge length. Tensile and bend tests were performed in an Instron machine at a constant cross-head speed of 1.26 mm/min. Axial strains were measured with a clip gauge attached to the 25 mm center portion of the specimen gauge length. For each volume fraction, the strengths of five specimens were measured. Whenever possible, broken composite specimens were examined by light and scanning electron-microscopy to determine the mode of failure.

RESULTS

Microstructure and Density

A typical cross section of a composite specimen with the excess outer matrix layers is shown in figure 2. In all composite specimens, mechanical polishing resulted in erosion of the matrix faster than the fiber. Because of this, a high magnification photograph of the fiber/matrix interface could not be taken. The composite matrix displayed density variations and significant porosity. Average density and porosity data in the green state and after nitridation for the 23 and 40 vol % SiC fiber/RBSN and for the unreinforced RBSN prepared under similar conditions are listed in table III. The composites

showed nearly 40 vol % porosity. X-ray analysis of composites after nitridation revealed a small amount of excess silicon (6 to 8 percent) in addition to approximately 60 percent αSi_3N_4 and approximately 32 percent βSi_3N_4.

Composite Properties

Axial bend and tensile strength. - the room temperature ultimate strength results for the 23 and 40 vol % SiC/RBSN composites are shown in table IV. Also included in the table for comparison purposes are the four-point bend strength data of unreinforced RBSN fabricated under similar processing conditions. The table also shows the influence of (L/h) ratio on four-point bend strength. Part of the scatter in strength data seen in the table can be attributed to a small variation in fiber volume fraction (±3 percent). In general, the data indicates that ultimate fracture strengths of the composites were significantly higher than those of the unreinforced RBSN matrix and that composite strengths increased with increase in fiber volume fraction.

Typical load-displacement behavior for a composite in a three-point bend test at room temperature is shown in figure 3. This specimen contained 20 vol % SiC fibers. In general, the load displacement curve showed two distinct regions. Initially, load increased linearly with displacement up to a stress level of 238 MPa. Above this stress level, the load-displacement curve was no longer linear. This nonlinear behavior appears to originate with the onset of matrix cracking normal to the fiber reinforcement direction. In figure 4, photograph of the tensile surface of a specimen stressed beyond the linear region reveals the formation of multiple matrix cracks. These cracks did not exist at any stress level below nonlinear region and initiated on the specimen surface where the tensile stress was maximum. As the sample was stressed to higher stress levels, more matrix cracks appeared at regular spacing. For a given fraction of fiber loading, both four-point and three-point bend specimens displayed similar average matrix crack spacings. The crack spacing was observed to vary with the matrix density, processing temperature, and fiber volume fraction. Data for the average matrix crack spacing and the composite stress at which the matrix first cracks are given in table V for the 23 and 40 vol % SiC/RBSN. With continued stressing, the composite reached its ultimate stress and broke noncatastrophically due to random fracture of the fibers.

The stress-strain behavior for a typical 20 vol % SiC/RBSN composite specimen tested in tension at room temperature is shown in figure 5. This figure is similar to that shown in figure 3 except for a second linear region after the nonlinear region. The deviation from linearity occurred at 220 MPa which is slightly lower than the stress level seen in figure 3. Above this stress level, audible noises were heard. It was not clear, however, whether these noises corresponded to matrix or fiber cracks. When the composite reached its ultimate strength, it broke noncatastrophically. In most tested specimens, fibrous fracture without complete separation of the specimen was observed. A specimen which was broken into two pieces, figure 6, displays the fibrous fracture. The matrix around the fiber fell apart due to high energy release at ultimate fracture.

Fiber/Matrix Interface

To evaluate the fiber-matrix interfacial bonding, a composite specimen was cut transversely to the fiber direction and tested in a three-point bend mode. The specimen containing 23 vol % SiC fiber showed a transverse bend strength of 76 MPa. The fracture surface, shown in figure 7, revealed that failure of the composite invariably occurred through a mechanism of interfacial splitting. The interfacial splitting occurred between the carbon-rich surface coating of the fiber and the matrix, indicating that the interfacial bonding was weak.

DISCUSSION

The results obtained in this study clearly demonstrate that reinforcement of RBSN by high strength, high modulus, large diameter (CVD) SiC fiber can yield a stronger and tougher (higher strain to failure) material than unreinforced RBSN. The mechanisms by which these improved properties occur can be analyzed from composite theory.

In general, when a ceramic matrix composite containing uniaxially aligned continuous ceramic fibers is stressed in tension in a direction parallel to the fiber, the composite extends elastically until one of the components fractures. The stress in the composite varies linearly with strain, and at any strain level the composite stress σ_c is given by

$$\sigma_c = \epsilon_c E_c = \epsilon_c (E_f V_f + E_m V_m) = \sigma_f V_f + \sigma_m V_m \qquad (1)$$

where σ is stress, ϵ is strain, E is modulus, V is volume fraction, and c, f, and m refer to composite, fiber, and matrix, respectively. The stress in each component will then be proportional to its modulus. The implicit assumptions of this equation are that the strain in the fiber, matrix, and composite are the same and that there is sufficient fiber-matrix bonding for load transfer.

In SiC/RBSN composites, the matrix is the weaker phase and cracks before the fibers. Therefore at matrix failure $\epsilon_c = \epsilon_m^f$ where ϵ_m^f is the matrix fracture strain. Substituting ϵ_m^f for ϵ_c in equation (1) and rearranging, the matrix fracture strain can be calculated.

$$\epsilon_m^f = \frac{\sigma_c^f}{(E_f V_f + E_m V_m)} \qquad (2)$$

where σ_c^f represents the composite stress at which the matrix first cracks. The matrix modulus E_m varies, however, with the volume fraction of porosity but can be estimated from the equation

$$E_m = 300 \exp(-3P) \text{ GPa} \qquad (3)$$

where P is volume fraction of porosity (ref. 10). For P ~0.39 typically measured for the RBSN matrix (cf. table III), the estimated value of E_m was 93 GPa. For the calculation of ϵ_m^f, the values of E_f = 390 GPa (ref. 11), E_m = 93 GPa and the appropriate values of σ_c^f corresponding to two different volume fractions were used (cf. table V). The calculated matrix fracture

strain values for the 23 and 40 vol % SiC/RBSN composites were 0.15 percent and 0.14 percent, respectively. These matrix strain values are comparable with the value of 0.11 percent obtained for unreinforced RBSN. This indicates that reinforcement of RBSN by large diameter SiC fibers did not significantly affect matrix failure strain. This is in contrast to the microcrack bridging effect (ref. 1) seen in small diameter SiC fiber or graphite fiber-reinforced glass composites (ref. 3). The implication of this finding is that the CVD SiC fibers have a diameter approximately equal in size or larger than the size of critical strength-controlling flaws in the RBSN.

Although the microcrack bridging mechanism is probably not operative with the large diameter SiC fibers, from equation (2) there are other methods available for increasing σ_c^f, the composite stress at which the first matrix crack appears. One method is by decreasing matrix porosity which will not only increase E_m (cf. eq. (3)), but also increase ϵ_m^f (ref. 10). Another method is by increasing the volume fraction of fibers. Assuming RBSN matrix with E_m = 206 GPa and ϵ_m^f = 0.15 percent i.e., (porosity 20 percent), the composite stress at which matrix cracks first occur was calculated for 50 vol % SiC/RBSN to be σ_c^f = 447 MPa which is significantly higher than the 300 MPa typical strength of RBSN with 20 percent porosity. This analysis shows that, even without microcrack bridging, reinforcement of RBSN by high modulus, high strength, large diameter SiC fibers can yield a stronger material whose properties can be tailored to suit a variety of design strength requirements.

After the first macrocrack in the matrix is formed, the load carried by the matrix will be transferred to the fiber and equation (1) is no longer valid. As the composite is loaded further, more matrix cracks appear and this process continues until the matrix effectively no longer bears any load. In this stage, the matrix is severely cracked while fibers are still intact. Thus the fibers impart the composite with higher toughness as manifested by noncatastrophic failure upon matrix cracking and a higher total strain capability. In contrast, in unreinforced RBSN, once a crack initiates, the material fails catastrophically at low strain. In some cases, however, multiple cracking of the matrix may not be desirable from a practical point of view because it may result in exposure of the fibers to the environment which at high temperature may promote severe loss in fiber strength. Therefore after initiation of the first matrix crack, usefulness of the composite may be lost.

With continued stressing, the fiber bundle will elongate until its failure stress is reached. Because SiC fiber is elastic up to failure, a second linear region is observed in the stress-strain curve. In fact, the ultimate tensile strength of the composite is a measure of the bundle strength of the fibers. When the matrix is completely cracked and carries no load, equation (1) reduces to

$$\sigma_c^u = \sigma_f^u V_f \tag{4}$$

where σ_c^u is the ultimate composite stress and σ_f^u represents the bundle strength of the fibers. Using the UTS values reported in table IV, the bundle strength calculated from equation (4) was 1.43 GPa. This value is less than the value 2.0 GPa, measured for the room temperature bundle strength of untreated, as-received fibers at a gauge length of 50 mm. It is also less than the 2.41 GPa value measured for the average room temperature tensile strength of SiC fibers heat treated in the nitriding furnace under similar

processing conditions as that of the composites. These results suggest fiber strength degradation may have occurred during processing of the composite.

Interfacial Shear Strength

The shear strength τ between the SiC fiber and the RBSN matrix can be estimated from the equation

$$\tau = \frac{\sigma_c^f D}{2.98 x V_f \left(1 + \frac{E_f V_f}{E_m E_m}\right)} \quad (5)$$

where σ_c^f is the composite stress corresponding to the first matrix crack, x is the mean separation between the matrix cracks, D is the fiber diameter and other terms have their usual meaning (refs. 1 and 12).

Using the values of x and σ_c^f from table V. The calculated mean interfacial strength was 10 MPa. This low value of shear strength is consistent with interfacial splitting observed on the fracture surface of the transverse flexural test specimen. A possible mechanism for low τ is the radial shrinkage of the fiber away from the matrix which can occur on cooling from the processing temperature due to a difference in fiber-matrix thermal expansion.

SUMMARY OF RESULTS

A fabrication method for reinforcing a powder-derived ceramic matrix with ceramic fibers has been developed. Using this method, 23 and 40 percent SiC fiber-reinforced RBSN composites have been fabricated. Initial room temperature properties for this composite have been evaluated. The important findings are as follows.

1. Room temperature strength measurements show that the axial tensile and flexural strengths increased with volume fraction of fibers and were significantly higher than unreinforced RBSN matrix of comparable porosity.

2. The composite matrix crazed before final fracture. The composite stress at which matrix first cracks increased with increasing volume fraction of fiber and was significantly greater than the fracture strength of unreinforced RBSN of the same porosity. This effect is primarily due to the higher modulus of CVD SiC fiber.

3. Due to their large diameter, the CVD SiC fibers did not measurably affect the matrix failure strain; however, due to their high strength and strength retention during processing, the CVD fiber allowed the composite to display extensive matrix cracking and high ultimate fracture strain, an indication of a tough material.

4. The composite displayed weak fiber-matrix bonding which resulted in low interfacial shear and low transverse flexural strength. Microstructural examination of the cross section of the composite indicates little evidence of the reaction between the fiber and the matrix.

5. Physical property measurements indicate that the composites have density values of 2.19 - 2.36 gm/cc and contain ~40 percent matrix porosity.

REFERENCES

1. J. Aveston, G.A. Cooper, and A. Kelley, "The Properties of Fiber Composites" Conference Proceedings, National Physical Laboratory (IPC Science and Technology Press Ltd, 1971) Paper I, p. 15.

2. J. Aveston and A. Kelley, "Theory of Multiple Fracture of Fibrous Composites," (1973), J. Mat. Sci., (8), p. 352.

3. J.J. Brennan and K.M. Prewo, "Silicon Carbide Fiber Reinforced Glass-Ceramic Matrix Composites Exhibiting High Strength and Toughness," (1982), J. Mat. Sci., (8), p. 2371.

4. F.W. Wawner, A.Y. Feng, and S.R. Nutt, "Microstructural Characterization of SiC (SCS) Filaments," (1983), SAMPE Q., (4), p. 39.

5. R.A. Signorelli, "Metal Matrix Composites for Aircraft Propulsion Systems," (1976), Proceedings of the 1975 International Conference on Composite Materials, edited by E. Scala, E. Anderson, I. Toth, and B.R. Norton, The Metallurgical Society AIME, New York, (1) p. 411.

6. R.T. Bhatt, "Fabrication of Continuous Fiber Reinforced Ceramic Composites," to be published.

7. T.P. Herbell, T.K. Glasgow, and N.J. Shaw, "Reaction Bonded Silicon Nitride Prepared from Wet Attrition Milled Silicon," (1980), NASA TM-81428.

8. J.A. Mangels, "Strength-Density-Nitriding Cycle Relationships for Reaction-Sintered Si_3N_4 in Nitrogen Ceramics," (1977), p. 569, edited by F.L. Riley, Noordhoff, Leyden, Netherlands.

9. C.P. Gazzara and D.R. Messler, "Determination of Phase Content of Si_3N_4 by X-Ray Diffraction Analysis," (1977), Am. Ceram. Soc. Bull. 56(9) p. 777.

10. A.J. Moulson, "Reaction-Bonded Silicon Nitride, Its Formation and Properties," (1979), J. Mat. Sci., (14) p. 1017.

11. J.A. DiCarlo and W. Williams, "Dynamic Modulus and Damping of Boron, Silicon Carbide, and Alumina Fibers," (1980), NASA TM-81422.

12. A.C. Kimber and J.G. Keer, "On the Theoretical Average Crack Spacing in Brittle Matrix Composites Containing Continuous Aligned Fibers," (1982), J. Mat. Sci. letters (1) p. 353.

TABLE I.- TRACE IMPURITY ANALYSIS OF AS-RECEIVED SILICON POWDER

ELEMENTS	wt. %
ALUMINUM	0.17
CALCIUM	0.02
CHROMIUM	0.06
IRON	0.53
MANGANESE	0.05
TITANIUM	0.03
VANADIUM	0.02
ZIRCONIUM	0.02

TABLE II. CHEMICAL ANALYSIS, SURFACE AREA AND AVERAGE PARTICLE SIZE OF SILICON POWDER

MATERIAL	OXYGEN, wt%	CARBON, wt%	NITROGEN, wt%	IRON, wt%	SURFACE AREA, m^2/g	AVERAGE PARTICLE SIZE, μm
AS-RECEIVED SILICON POWDER	0.43	0.025	0.0004	0.60	1.644	6.0
ATTRITION MILLED SILICON POWDER	1.20	0.31	0.07	0.60	10.216	0.4

TABLE III. DENSITY AND POROSITY DATA FOR SiC/RBSN COMPOSITES

VOLUME FRACTION OF FIBERS	BEFORE NITRIDATION		AFTER NITRIDATION	
	DENSITY gm/cc	MATRIX POROSITY, %	DENSITY gm/cc	MATRIX POROSITY, %
0	1.56	35	1.98	37
23 ± 3	1.70	54[a]	2.19	39[a]
40 ± 2	1.90	51[a]	2.36	40[a]

a. Matrix porosity calculated from composite density and from theoretical density for CVD SiC fiber (3.0 gm/cc) and from density for silicon (2.4 gm/cc) or for Si_3N_4 (3.2 gm/cc).

TABLE IV.- ROOM TEMPERATURE STRENGTHS OF RBSN AND AND SiC RBSN COMPOSITES

TEST	AXIAL STRENGTH, MPa		
	0° FIBER	23 ± 3° FIBER	40 ± 2° FIBER
4 POINT BEND ($\frac{L}{h}$ = 15)[a]	107 ± 26[c]	539 ± 48[c]	616 ± 36[c]
4 POINT BEND ($\frac{L}{h}$ = 45)	-------	675 ± 42	868 ± 32
3 POINT BEND ($\frac{L}{h}$ = 35)	-------	717 ± 80	958 ± 45
TENSILE[b]	-------	352 ± 73	536 ± 20

a. $\frac{L}{h}$ refers to span to height ratio of test specimen. h = 1.2 mm
b. Tested at 50 mm gauge length
c. Standard deviation for five tests

TABLE V.- MEAN MATRIX CRACK SPACING AND FIRST CRACKING STRESS FOR SiC/RBSN COMPOSITES

FIBER FRACTION, %	MATRIX CRACK SPACING, mm	COMPOSITE STRESS AT WHICH MATRIX FIRST CRACKED, MPa
23±3	2.0±0.3[a]	237±25[b]
40±2	0.9±0.2	293±15

a. Standard deviation for 30 cracks on five bend specimens.
b. Standard deviation for 5 specimens measured in 3-point bend.

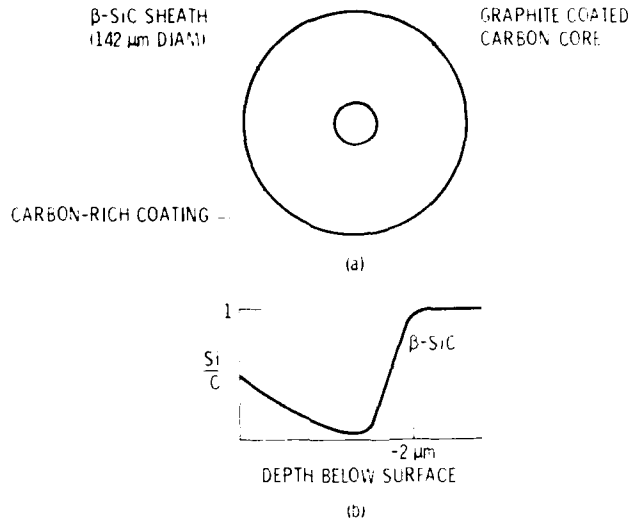

Figure 1. (a) Schematic of cross section of CVD SiC fiber.
(b) The composition profile of carbon-rich coating on the surface of SiC fiber (AVCO SCS-6 fiber).

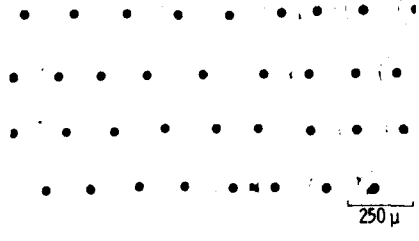

Figure 2. - A typical cross section of SiC/RBSN composite showing fiber distribution.

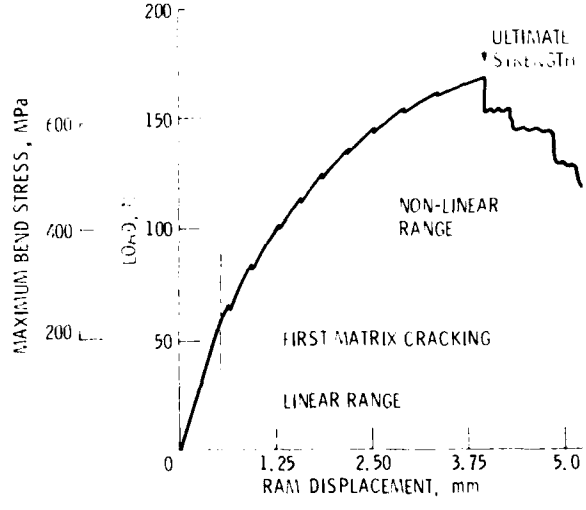

Figure 3. - The load-deflection behavior in 3-point bending for 20 vol% SiC fiber/RBSN composite

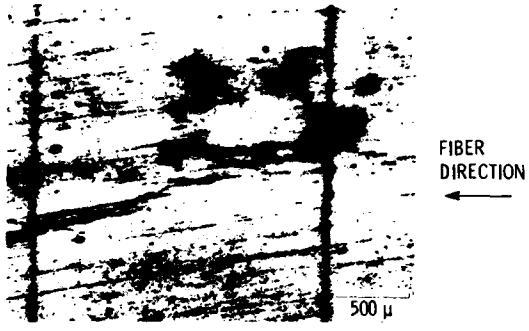

Figure 4. - A typical 3-point bend specimen stressed above the non-linear range showing matrix cracks normal to fibers on the tensile surface.

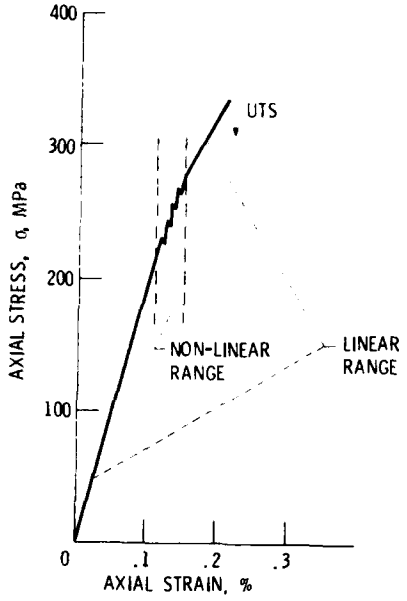

Figure 5. - The tensile stress-strain behavior for 20 vol% SiC fiber /RBSN composite showing linear and non-linear ranges.

Figure 6. - A fractured tensile specimen showing fibrous fracture and fiber pull out.

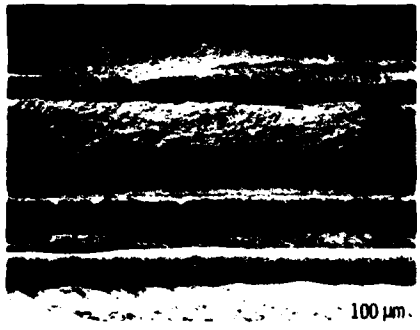

Figure 7. - Fracture surface of a 23 vol% SiC/RBSN composite tested in transverse flexure showing interfacial splitting between fiber and matrix.

1. Report No. NASA TM-87085 USAAVSCOM-TR-85-C-14	2. Government Accession No. AD-A160622	3. Recipient's Catalog No.

4. Title and Subtitle	5. Report Date
Mechanical Properties of SiC Fiber-Reinforced Reaction-Bonded Si_3N_4 Composites	6. Performing Organization Code 533-05-12
7. Author(s) Ramakrishna T. Bhatt	8. Performing Organization Report No. E-2671
	10. Work Unit No.
9. Performing Organization Name and Address NASA Lewis Research Center and Propulsion Directorate U.S. Army Aviation Research and Technology Activity (AVSCOM), Cleveland, Ohio 44135	11. Contract or Grant No
	13. Type of Report and Period Covered Technical Memorandum
12. Sponsoring Agency Name and Address National Aeronautics and Space Administration Washington, D.C. 20546 and U.S. Army Aviation Systems Command, St. Louis, Mo. 63120	14. Sponsoring Agency Code

15. Supplementary Notes

Prepared for the 21st University Conference on Ceramic Science, sponsored by The Pennsylvania State University, University Park, Pennsylvania, July 17-19, 1985.

16. Abstract

The room temperature mechanical and physical properties of silicon carbide fiber-reinforced reaction-bonded silicon nitride composites (SiC/RBSN) have been evaluated. The composites contained 23 and 40 volume fraction of aligned 140 μm diameter chemically vapor deposited SiC fibers. Preliminary results for composite tensile and bend strengths and fracture strain indicate that the composites displayed excellent properties when compared with unreinforced RBSN of comparable porosity. Fiber volume fraction showed little influence on matrix first cracking strain but did influence the stresses required for matrix first cracking and for ultimate composite fracture strength. It is suggested that by reducing matrix porosity and by increasing the volume fraction of the large diameter SiC fiber, it should be possible to further improve the composite stress at which the matrix first cracks.

17. Key Words (Suggested by Author(s))	18. Distribution Statement
Fiber-reinforced composites; SiC fiber; Si_3N_4 matrix; Mechanical properties	Unclassified - unlimited STAR Category 24

19. Security Classif. (of this report)	20. Security Classif. (of this page)	21. No. of pages	22. Price*
Unclassified	Unclassified		

*For sale by the National Technical Information Service, Springfield, Virginia 22161

END

FILMED

12-85

DTIC